NASA Technical Memorandum 79297

ATOMIZING CHARACTERISTICS OF SWIRL CAN COMBUSTOR MODULES WITH SWIRL BLAST FUEL INJECTORS

Robert D. Ingebo
Lewis Research Center
Cleveland, Ohio

Prepared for the
Twenty-fifth Annual International Gas Turbine Conference
sponsored by the American Society of Mechanical Engineers
New Orleans, Louisiana, March 9-13, 1980

ATOMIZING CHARACTERISTICS OF SWIRL CAN COMBUSTOR MODULES WITH SWIRL BLAST FUEL INJECTORS

Robert D. Ingebo
National Aeronautics and Space Administration
Lewis Research Center
Cleveland, Ohio

ABSTRACT

Cold flow atomization tests of several different designs of swirl can combustor modules were conducted in a 7.6 cm diameter duct at airflow rates (per unit area) of 7.3 to 25.7 g/cm^2 sec and water flow rates of 6.3 to 18.9 g/sec. The effect of air and water flow rates on the mean drop size of water sprays produced with the swirl blast fuel injectors were determined. Also, from these data it was possible to determine the effect of design modifications on the atomizing performance of various fuel injector and air swirler configurations. The trend in atomizing performance, as based on the mean drop size, was then compared with the trends in the production of nitrogen oxides obtained in combustion studies with the same swirl can combustors. It was found that the fuel injector design that gave the best combustor performance in terms of a low NO_x emission index also gave the best atomizing performance as characterized by a spray of relatively small mean drop diameter. It was also demonstrated that at constant inlet airstream momentum the nitrogen oxides emission index was found to vary inversely with the square of the mean drop diameter of the spray produced by the different swirl blast fuel injectors. Test conditions were inlet-air static pressures of 1×10^5 to 2×10^5 N/m^2 at an inlet-air temperature of 293 K.

INTRODUCTION

An investigation was conducted to determine how the mean drop size of fuel sprays might be related to the concentration of oxides of nitrogen produced by swirl can combustor modules. Previous experimental high pressure combustor tests have shown that the nitrogen oxide emission index (NO_xEI) was lower with swirl blast (air atomizing) than with simplex (pressure atomizing) fuel injectors, at combustor inlet-air pressures of 20 atmospheres (ref. 1). This was attributed to improved atomization obtained with the swirl blast or air atomizing type fuel injector. However, drop size data were not available for the injectors so it was impossible to determine the effect of injector performance on emission data. Also, in references 2 and 3, NO_xEI data were obtained for several different designs of swirl can combustor modules with swirl blast fuel injectors. However, atomizer performance data were again lacking. Thus, the present investigation was undertaken to obtain atomizer performance data for several different types of fuel injector and airswirlers used in reference 2. Such data could then be used to demonstrate how atomizer performance might be related to NO_xEI data reported in reference 2.

The mean drop size of water sprays produced by swirl blast fuel injectors in swirl can combustor modules were determined from tests in high velocity airstreams. The aerodynamic force of the airstream and the liquid flow rate were varied to determine their respective effects on spray mean drop sizes produced with each of five different swirl can designs. From these data, it was possible to evaluate and compare atomizer performance. Such data are needed to design fuel injectors that will reduce exhaust emissions and enhance combustor performance. A scanning radiometer was used to obtain mean drop diameter data for each spray produced by the swirl blast fuel injectors.

To evaluate the atomizing performance of each swirl blast fuel injector, cold flow tests were conducted at air flow rates (per unit area) of 7.3 to 25.7 g/cm^2 sec and water flow rates of 6.3 to 18.9 g/sec. Test conditions included inlet-air static pressures of 1×10^5 to 2×10^5 N/m^2 at an inlet-air temperature of 293 K.

APPARATUS AND PROCEDURE

As shown in figure 1, air drawn from the laboratory supply system was at ambient temperature (293 K), and pressures in the test section were varied from 1×10^5 to 1.98×10^5 N/m^2. Airflow rate was controlled with a valve directly downstream of the air orifice. The test section consisted of a 7.6 cm inside diameter duct 15.2 cm in length and mounted, with a bellmouth, inside of a 15.2 cm inside diameter duct 5 m in length. The airswirler at the exit of the swirl-can combustor module was mounted in the same plane as the duct exit and at a distance of 11.4 cm upstream of the centerline of the 7.5 cm diameter laser light field. A scanning radiometer was mounted near the end of the open duct test facility.

SCANNING RADIOMETER

The scanning radiometer, shown in figure 2, was used to determine the mean drop size of water sprays produced at each test condition. The optical system shown in figure 2 consisted of a 1 mW helium-neon laser, a 0.003 cm diameter aperture, a 7.5 cm diameter collimating lens, a 10 cm diameter converging lens, a 5 cm diameter collecting lens, a scanning disk with a 0.05 × 0.05 cm slit, a timing light and a photomultiplier detector. A complete description of the scanning radiometer and the method of determining mean drop diameters are given in reference 4. Calibration tests of the instrument were performed as discussed in reference 5.

SWIRL-CAN COMBUSTOR MODULES

Design configurations of the five swirl-can combustor modules, Models 2, 8, 9, 10, and 11 of reference 2, tested to determine their atomizing performance are shown in figure 3. Model 2 consisted splash plate fuel injector and a single airswirler with twelve, 45 degree angle, blades. The liquid sheet broken up by the airstream just upstream of the airswirler. Model 8 was similar to Model 2 except that a second concentric airswirler was used to give a contraswirl to the airstream around the inner airswirler. In Model 9, the two concentric airswirlers were the same as Model 8. However, the splash plate fuel injector consisted of a disk mounted 0.15 cm downstream of the airswirlers to produce liquid sheet breakup with swirling airflow. Model 10 was similar to Model 9 except that the two concentric airswirlers were both mounted flush with the combustor module exit. Model 11 was similar to Model 8 with two concentric airswirlers mounted at the combustor module exit. However, the fuel injector consisted of a 0.051 cm circumferential slot in the end of the fuel tube, and the fuel-air mixture passed through an annular slot with an open area of 0.70 cm^2. A brief description of airswirler characteristics and fuel injector location is given in Table I, and a more detailed description of airswirlers and fuel injection techniques is given in reference 2.

RESULTS AND DISCUSSION

The atomizing performance of each combustor module was determined by obtaining mean drop size data which was then related to NO_xEI values previously obtained in reference 2. Also, combustor module performance results were analyzed to determine effects of recirculation or primary zone mixing on NO_xEI.

Effect of Airstream Momentum on Mean Drop Size

Mean drop diameters were determined for sprays produced by the five different types of swirl can combustor modules shown in figure 3. Model 2 was the first type tested. It consisted of a liquid jet impinging on the upstream hub of a single airswirler. The effects of airstream momentum (ρV) on mean drop diameter, at water flow rates of 6.3 and 18.9 g/sec, is shown in figure 4. The higher water flow rate, 18.9 g/sec, gave a somewhat smaller mean drop diameter than the lower water flow rate. This was attributed to a possible increase in the radial penetration of the liquid thereby producing an increase in surface area of the liquid across the airswirler. High liquid pressure drop across the orifice at high liquid flow rates would also tend to decrease mean drop size. This is an interesting result since increasing the liquid flow rate usually increases the mean drop size in the case of breakup of liquid conical sheets produced by pressure atomizing (simplex) nozzles. Figure 4 also shows that mean drop size varied with airstream momentum $(\rho V)^{-0.5}$ and $(\rho V)^{-0.4}$ at high and low liquid flow rates, respectively.

The next swirl can combustor module tested was Model 8 with the liquid jet impinging on the upstream face of the hub of two contraswirl concentric airswirlers. The performance obtained with the Model 8 atomizer is shown in figure 5. Again, due to improved radial liquid penetration which increased liquid surface area, a higher water flow rate gave a somewhat smaller mean drop size which varied inversely with the square root of the airstream momentum, $(\rho V)^{-0.5}$. Also, the mean drop size was approximately 20 percent greater than that obtained with Model 2 under similar air and water flow rate conditions. This was attributed to poorer breakup being obtained with Model 2 due to the outer contraswirler tending to reduce the break-up effectiveness of the inner contraswirler.

Model 9 was similar to Model 8 with two contraswirl concentric airswirler mounted at the swirl can exit. However, the splash plate fuel injector consisted of a disk mounted 0.15 cm downstream of the downstream face of the hub so that the liquid sheet was produced downstream of the airswirler. The results obtained by injecting fuel downstream of the airswirlers with Model 9, are shown in figure 6. Mean drop diameters were somewhat larger than those obtained with Model 2. This was attributed to the loss of airstream momentum in passing through the airswirler prior to atomizing the liquid. Also, a water flow rate of 12.6 gave mean drop sizes intermediate between the high and low water flow rates. Reasons for this are the same as those already given for Models 2 and 8.

Model 10 was designed similar to Model 9 except that the two concentric airswirlers were mounted in the same plane at the combustor module exit instead of having the inner swirler recessed 0.56 cm upstream of the swirl can exit. As shown in figure 7, mean drop diameters obtained for three water flow rates were somewhat larger for Model 10 than those obtained with Model 9. This was attributed to the outer contraswirl canceling out some of the momentum of the inner contraswirl when the two airswirlers were mounted flush, as was the case with Model 9. Also, the mean drop size varied inversely with the square root of the airstream momentum (ρV), at a water flow rate of 18.9 g/sec.

The final configuration tested (Model 11) was similar to Model 8 with two concentric airswirlers mounted at the combustor module exit. However, the fuel injector was quite different. Liquid fuel was sprayed into the airstream through a 0.051 cm circumferential slot in the end of the fuel tube. The mixture of fuel and air then passed through an annular slot having an open area of 0.70 cm^2. Mean drop diameters, as shown in figure 8, were considerably larger for Model 11 than those obtained with the other four models. However, mean drop diameters were again found to vary inversely with the square root of the airstream momentum as observed with the other swirl can modules.

Relationship of Mean Drop Diameter to NO_xEI

Since a considerable variation in mean drop size was obtained with the five swirl can combustor modules, it might be assumed that the mean drop size could have some measurable effect on the concentration of nitrogen oxides produced by the five modules (Models 2, 8, 9, 10, and 11).

In reference 4, a theoretical study of the formation of nitric oxide in burning fuel sprays, indicated that finer fuel sprays would produce less nitric oxide than coarse ones. To test this theoretical prediction, the variation in mean drop diameter obtained in this study is plotted against the NO_xEI data of reference 2 at constant values of ρV as shown in figure 9. These data show that, at constant inlet airstream momentum, the NO_xEI varied with the square of the mean drop diameter. This is in agreement with equations (24) and (25) in reference 6 which may be combined and rewritten as $\dot{M}_{NO}/\dot{M} \sim D^3/D$ for a single droplet diffusion flame where D is drop diameter, $\dot{M}_{NO}$ is the mass production rate of NO and $\dot{M}$ is the mass burn-

ing rate. Thus, for a spray of fuel drops it may be assumed that $NO_xEI \sim (\Sigma_n D^3/\Sigma_n D) \sim D_{31}^2 \sim D_m^2$ where NO_xEI is grams of oxides of nitrogen produced per kilogram of fuel, D_{31} is the volume to diameter mean, and D_m is the mean drop diameter measured with the light scattering instrument. Also it is interesting to note in figure 9 that, for a given model, NO_xEI increased as ρV increased even though D_m decreased. Thus, NO_xEI was controlled more by aerodynamic mixing and reaction kinetics than by D_m.

Since water was used in this study to simulate Jet A fuel, the effect of liquid properties should be considered in evaluating D_m. As shown in the comparison of liquids in Table II, $D_{mf}^2 \sim (\nu^*\sigma^*)^{0.5} \times D_{mw}^2$, where D_{mf} and D_{mw} are mean drop diameters of fuel and water, respectively. ν^* and σ^* are normalized kinematic viscosity and surface tension, respectively. The exponent 0.5 for the term $\nu^*\sigma^*$ was taken from reference 7 where it was found that $D_{30} \sim (\nu\sigma)^{1/4}$ which was in fair agreement with the exponent of 1/3 given in reference 8 for capillary liquid breakup. As shown in Table II, the value of D_{mf}^2 for Jet A fuel was only 8 percent less than D_{mw}^2. This indicates that water gave a fair simulation of Jet A fuel. Also, fuel flow rates were simulated with water flow rates as given in Table III.

Effect of Recirculation Zone Design on NO_xEI

A general expression for the formation of nitrogen oxides produced by diffusion flame burning of a fuel spray may be written as follows:

NO_xEI = f (mean drop size of the spray), (turbulent mixing of fuel and air), (reaction kinetics of NO_x formation)

where each term in the brackets is a function of combustor pressure (δ). Thus, when the inlet air temperature, fuel-air ratio and combustor reference velocity are constant, the equation may be rewritten as:

$$NO_xEI \sim \delta^x = f(\delta^d, \delta^t, \delta^r) = f(\delta^d, \delta^a)$$

where δ^x is the total effect of pressure, that is, $x = d + a$, and $a = t + r$, and δ^d is the affect of pressure due to drop size. Since it is beyond the scope of this study to isolate the effect of pressure due to turbulent mixing, δ^t, and reaction kinetics, δ^r, the pressure exponent a is assumed for the product of the two factors, δ^a.

To evaluate the exponent a, the equation may be rewritten as:

$$NO_xEI/D_m^2 \sim \delta^a$$

since $a = x - d$. Thus, as shown in figure 10, the parameter NO_xEI/D_m^2 is plotted against δ for constant values of fuel-air ratio, inlet-air temperature and reference velocity as given in Table III.

Over the range of $\delta = 6.5$ to 13, values of the exponent a are given in Table IV for the five combustor modules as well as values of x which are compared with those obtained in reference 2. For Model 9, the agreement is fairly good, that is, $x = 0.7$ from figure 10 and $x = 0.74$ in reference 2. Also, Model 9 gave the lowest value of the parameter NO_xEI/D_m^2 whereas Model 8 gave the largest value, at $\delta = 6.5$. This is attributed to the fact that Model 9 was designed "to confine fuel to (the) recirculation zone better than Model 8," as stated in reference 2. Thus, a reduction in the parameter NO_xEI/D_m^2 indicated improved turbulent mixing in the recirculation zone.

It is interesting to note that although Model 2 gave the smallest mean drop size of all of the models yet it did not have as low a value of NO_xEI/D_m^2 as might be expected. This was attributed to relatively poor turbulent mixing. When fuel was injected upstream of the airswirler, that is, Models 2 and 8, values of NO_xEI/D_m^2 were relatively large which was also due to poor turbulent mixing. Model 11 gave the next best performance based on the parameter NO_xEI/D_m^2, that is, approximately 24 percent higher than that of Model 9 at $\delta = 6.5$. Although Model 11 has a good recirculation zone, it gave coarser atomization than Model 9, and as a result had the highest NO_xEI values and largest mean drop sizes of all of the models tested. The poor atomization of Model 11 was attributed to its low blockage which was only 51.1 percent as compared with 60.3 percent for the other models, as shown in Table I.

At values of $\delta > 13$, there appeared to be a marked increase in the effect of δ on NO_xEI/D_m^2 and all models gave a value of approximately 25 at $\delta = 16.3$. Thus at this high pressure condition, factors such as injection upstream or downstream of the airswirler and the recirculation zone at the flame holder had little effect on NO_xEI/D_m^2. This indicates the need for more knowledge of the effect of combustor inlet-air pressure on fuel atomization, turbulent mixing and reaction kinetics at values of $\delta > 16$.

SUMMARY OF RESULTS

Atomizing performance tests of five differently designed swirl can combustor modules indicated that the mean drop diameter varied inversely with the square root of the airstream momentum (ρV) at the higher water flow rate (18.9 g/sec). At the lower water flow rate (6.3 g/sec), mean drop diameters were somewhat larger and gave slightly smaller variations with changes in airstream momentum. The Model 2 and Model 11 swirl can modules gave the smallest and largest mean drop sizes, respectively.

Comparison of the atomization results of this study and the combustion results of reference 2 indicated that Model 2 which gave the smallest mean drop diameters also gave the lowest nitrogen oxides emission index. Similarly, Model 11 gave the largest mean diameters and it produced the highest nitrogen oxides emission index. A comparison of the formation of NO_xEI with mean drop diameter indicated that NO_xEI was proportional to the mean drop diameter squared. This is in agreement with theoretical results given in reference 4 for the formation of nitric oxide in droplet diffusion flames.

The parameter NO_xEI/D_m^2 was found to be useful in comparing emissions of the five combustor modules. For a range of $\delta = 6.5$ to 13, the lowest values of NO_xEI/D_m were obtained with Model 9 which also gave the best aerodynamic mixing in the primary or recirculation zone.

REFERENCES

1 Ingebo, R. D., and Norgren, C. T., "High Pressure Combustor Exhaust Emissions with Improved Air Atomizing and Conventional Pressure Atomizing Fuel Nozzles," NASA TN D-7154, 1973.

2 Mularz, E. J., Wear, J. D., and Verbulecz, P. W., "Pollution Emissions from Single Swirl-Can Combustor Modules at Parametric Test Conditions," NASA TM X-3167, 1975.

3 Mularz, E. J., Wear, J. D., and Verbulecz, P. W., "Exhaust Pollutant Emissions from Swirl-Can Combustor Module Arrays at Parametric Test Conditions," NASA TM X-3237, 1975.

4 Buchele, D. R., "Scanning Radiometer for Measurement of Forward-Scattered Light to Determine Mean Diameter of Spray Particles," NASA TM X-3454, 1976.

5 Ingebo, R. D., "Effect of Airstream Velocity on Mean Drop Diameters of Water Sprays Produced by Pressure and Air Atomizing Nozzles," NASA TM-73740, 1977.

6 Bracco, F. V., "Nitric Oxide Formation in Droplet Diffusion Flames," Fourteenth Symposium (International) on Combustion, The Combustion Institute, 1973, pp. 831-842.

7 Ingebo, R. D., and Foster, H. H., "Drop-Size Distribution for Crosscurrent Breakup of Liquid Jets in Airstreams," NACA TM-4087, 1957.

8 Adelberg, M., "Mean Drop Size Resulting from the Injection of a Liquid Jet into a High-Speed Gas Stream, AIAA Journal, Vol. 6, No. 6, June 1968, pp. 1143-1147.

TABLE I. - AIRSWIRLER CHARACTERISTICS AND FUEL INJECTOR LOCATION

Airswirlers			
Model number	Percent blockage	Description	Fuel injector location
9	60.3	Double, contraswirl recessed inner swirl	Downstream of airswirler
11	51.1	Double, contraswirl	In center of airswirler
10	60.3	Double, contraswirl flush inner swirler	Downstream of airswirler
2	60.3	Single airswirler	Upstream of airswirler
8	60.3	Double, contraswirl recessed inner swirler	Upstream of airswirler

TABLE II. - LIQUID PHYSICAL PROPERTIES, AT 293 K

Liquid	ν, cm^2/sec	σ, N/m	$^a\nu^*$	$^b\sigma^*$	$\nu^*\sigma^*$	$(\nu^*\sigma^*)^{0.5}$
Kerosene	2.72	0.028	2.72	0.384	1.04	1.02
Jet A	2.18	.028	2.18	.384	.84	.92
Water	1.00	.073	1.00	1.000	1.000	1.000

$^a\nu^*$ = liquid/water, normalized kinematic viscosity.

$^b\sigma^*$ = liquid/water, normalized surface tension.

TABLE III. - SIMULATED COMBUSTOR CONDITIONS

ρV_{ref}, g/cm^2 sec (a)	δ, atm	$\dot{W}_{water}$, g/sec (b)
7.3	6.5	6.8
11.0	9.8	10.2
14.7	13.0	13.6
18.3	16.3	17.0

$^a V_{ref}$ = 23.2 m/sec, and ρ evaluated at T_a = 733 K.

$^b \dot{W}_{water} = (\rho_{water}/\rho_{fuel})\ (F/A)\dot{W}_{air}$, where fuel-air ratio, F/A = 0.02.

TABLE IV. - COMPARISON OF RESULTS WITH REFERENCE 2

($NO_xEI \sim \delta^x$)

Model number	NO_xEI/D_m^2		From figure 10 δ = 6.5 to 13		From reference 2
	δ = 6.5	δ = 16.3	a	x	x
9	3.8	26	1.7	0.7	0.74
11	4.7	25	1.6	.6	.70
10	4.7	27	1.6	.6	.66
2	4.9	24	1.6	.6	.61
8	5.7	26	1.5	.5	.37

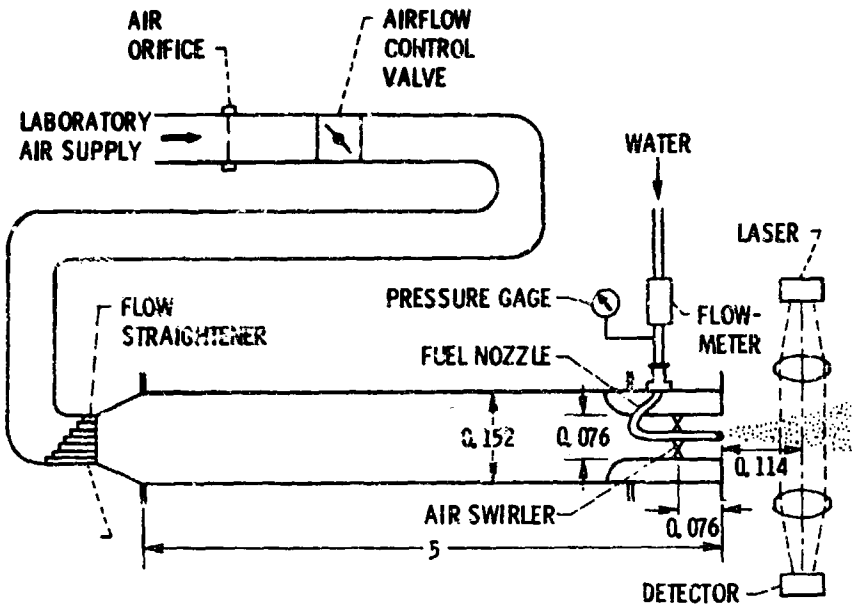

Figure 1. - Test facility and auxiliary equipment. (Dimensions are in meters.)

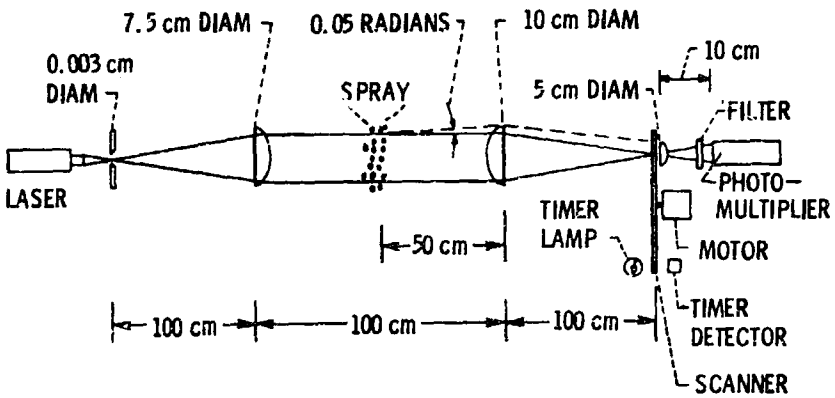

Figure 2. - Scanning radiometer optical path.

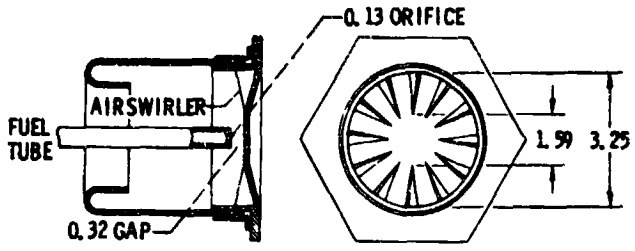

(a) MODEL #2 (SINGLE SWIRLER).

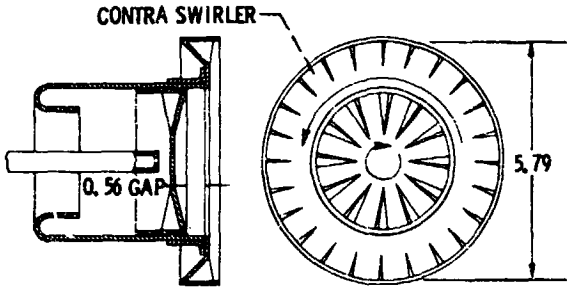

(b) MODEL #8 (INNER SWIRLER RECESSED).

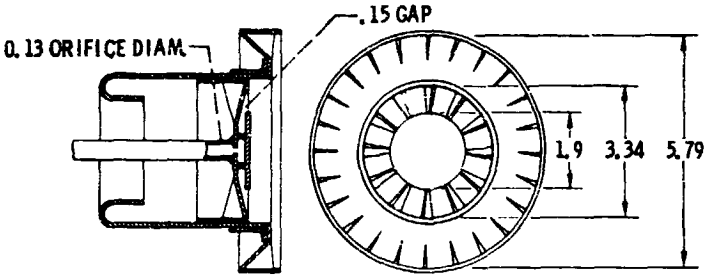

(c) MODEL #9 (INJECTION DOWNSTREAM OF SWIRLER).

(d) MODEL #10 (FLUSH MOUNTED SWIRLERS).

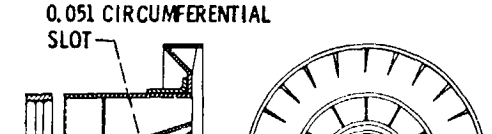

(e) MODEL #11 (FUEL-AIR PREMIXING).

SWIRL-CAN COMBUSTOR MODULE

Figure 3. - Swirl-can combustor modules (same as ref. 2, dimensions are in cm.).

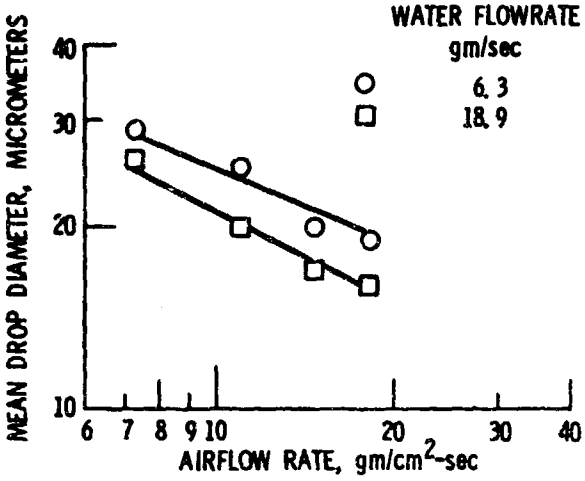

Figure 4. - Variation of mean drop diameter with airstream momentum with Model #2 swirl-can combustor module.

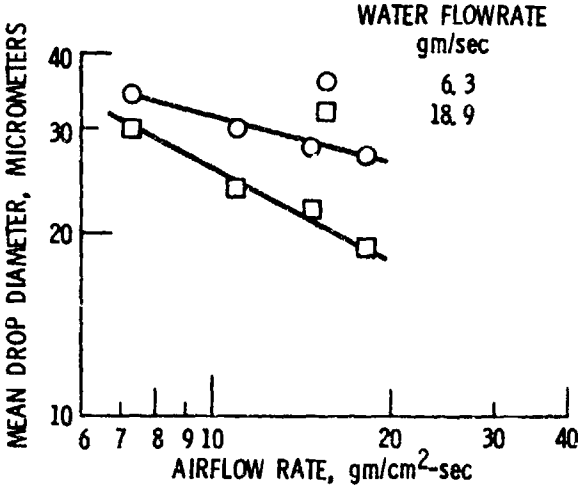

Figure 5. - Variation of mean drop diameter with airstream momentum with Model #8 swirl-can combustor module.

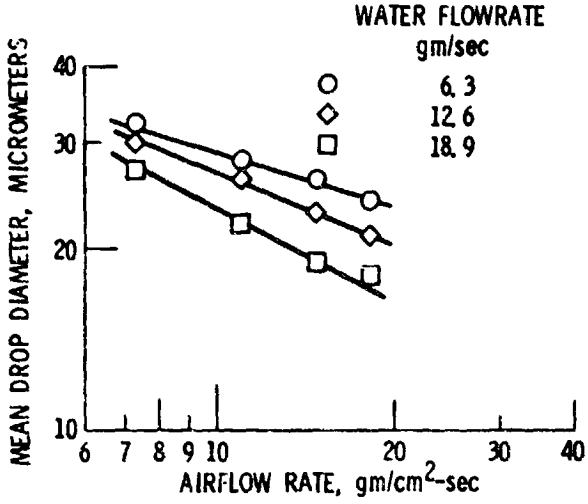

Figure 6. - Variation of mean drop diameter with airstream momentum with Model #9 swirl-can combustor module.

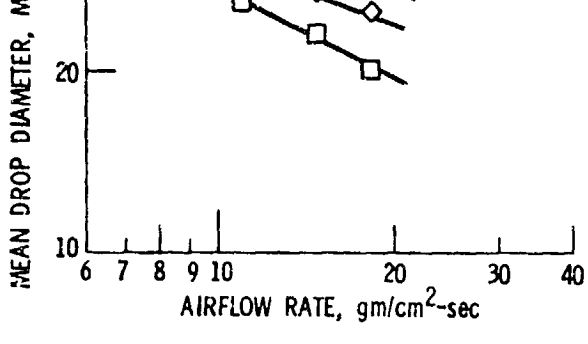

Figure 7. - Variation of mean drop diameter with airstream momentum with Model #10 swirl-can combustor module.

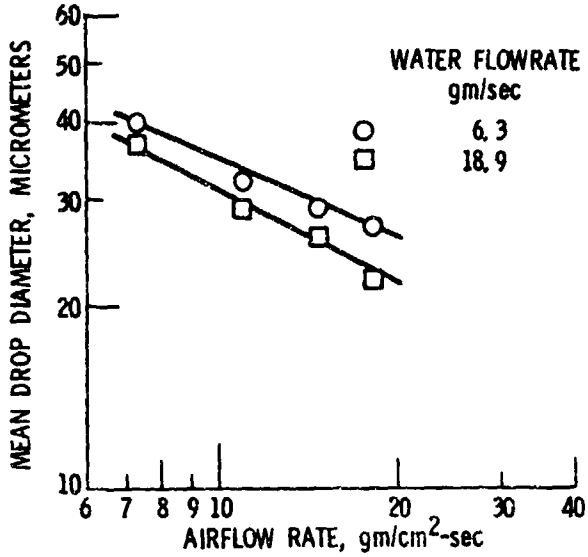

Figure 8. - Variation of mean drop diameter with airstream momentum with Model #11 swirl-can combustor module.

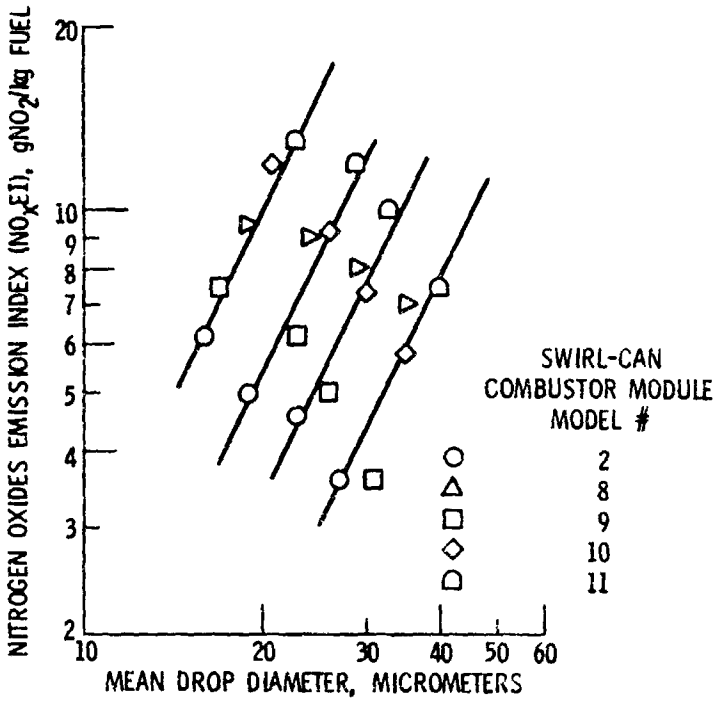

Figure 9. - Variation of NO_xEI with mean drop diameter with swirl-can combustor modules of reference 2.

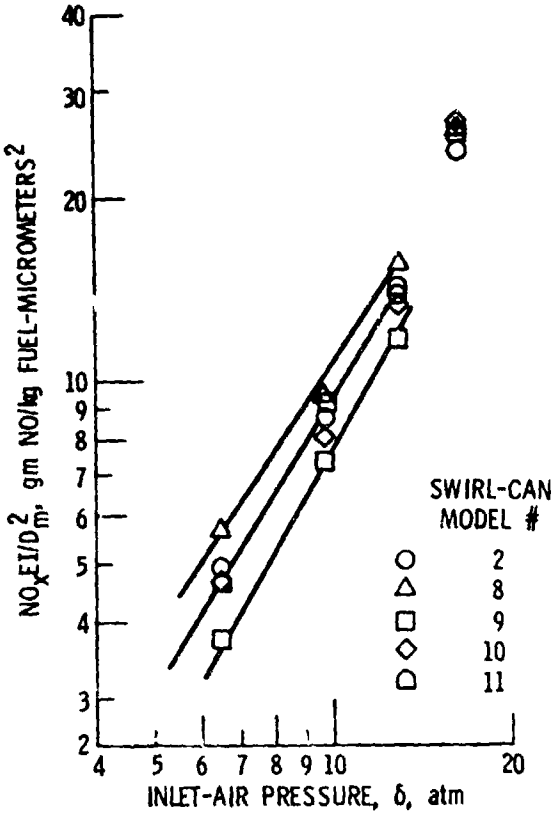

Figure 10. - Variation of $NO_x EI/D_m^2$ with inlet-air pressure, δ.